ICHE 2014, Hamburg - Lehfeldt & Kopmann (eds) - © 2014 Bundesanstalt für Wasserbau ISBN 978-3-939230-32-8

Numerical Study of Morphodynamics and Ecological Parameters Following Alternative Groyne Layouts at the Danube River

M. Tritthart, M. Glas, M. Liedermann & H. Habersack
Christian Doppler Laboratory for Advanced Methods in River Monitoring, Modelling and Engineering, Institute of Water Management, Hydrology and Hydraulic Engineering, University of Natural Resources and Life Sciences, Vienna, Austria

ABSTRACT: A numerical study of the impact of different groyne layouts and shapes on the flow field as well as morphodynamic and ecological conditions at the Danube River in Austria is presented. Two sections of the river, ranging between 3 and 4 km in length, served as study sites. In order to study their influence on hydrodynamics, morphodynamics and fluvial ecology, the parameters groyne length, groyne spacing, base shape and crest elevation were varied within reasonable bounds in a 3D numerical model. Moreover, the impact of groyne inclination was studied by investigating attracting, orthogonal and repelling groynes. It was found that an increase of the groyne length as well as a decrease of the groyne spacing lead to rising water levels. However, these measures also increase bedload transport rates, resulting in river bed erosion. Exchange processes between river and groyne fields are reduced, thus increasing water ages. In turn, sedimentation in the fairway is obtained by an increase of the groyne spacing and a reduction of the groyne length. This also corresponds to an increase of mass exchange between river and groyne fields due to the occurrence of two gyres. Moreover, it was found that the highest sensitivity of all groyne parameters in terms of morphodynamic processes is exhibited by the crest elevation. An optimization of the crest elevation is essential for achieving the aim of a dynamic equilibrium of the river bed.

Keywords: Numerical model, Sediment transport, Bed load, Groyne, Ecology, Danube River

1 INTRODUCTION

For centuries lateral structures in rivers have been used successfully mainly for the purpose of river training, in order to stabilize the river banks and to improve navigability where applicable. The first documented use of groynes in river engineering has been between 400 and 500 years before the present day (e.g. Vierlingh, 1576), with Leonado da Vinci being among the first to apply it, at the river Arno (Uijttewaal, 2005). Despite this long history of practical application, there is still relatively little knowledge about the precise mechanisms that are governing three-dimensional hydrodynamics, morphodynamics and ecological processes in groyne fields and the adjacent regions of the river cross section. Most river rehabilitation projects are therefore still carried out using a trial-and-error approach (Biron et al., 2005).

In recent years, studies on groyne-induced processes have been conducted on idealized structures both experimentally (e.g. Uijttewaal et al., 2001; Biron et al., 2005; Uijttewaal, 2005; Kang et al., 2011; Yossef and de Vriend, 2011) and numerically (Ouillon and Dartus, 1997; Alauddin and Tsujimoto, 2012). Actual field data of the Danube River were used for the calibration of a numerical particle tracing model in Tritthart et al. (2009), presenting a framework to study retention times in groyne fields. In Sukhodolov (2014) hydrodynamics and mixing processes in a river reach with groynes were studied in nature under semi-controlled conditions. Lechner et al. (2014) investigated dispersal patterns of fish larvae in the Danube River, thereby comparing the ecological functioning of shoreline configurations involving groynes to those without structural features. However, most studies so far considered only straight groynes in orthogonal or repelling layouts, since conventional wisdom holds that groynes need to guide the flow towards the center of the river in order to protect the river banks. Only in the past few years, alternative groyne types were tested in practice. For example, innovative groyne types and the difference to orthogo-

nal groynes in terms of hydrodynamics and morphodynamics were studied recently in the field at the river Elbe (Henning and Hentschel, 2013). Alternative groyne layouts may involve attracting groynes, which guide the flow towards the bank to deliberately induce lateral erosion, in order to reduce the sediment deficit that many rivers are facing today. Other innovative groyne types include curved structures, which create specific habitats on their leeside or lowered groyne bases, which increase the flow in the groyne fields.

In this paper, at the example of the Danube River, we investigate numerically the influence of several groyne parameters on hydrodynamics, morphodynamics and ecological functioning of the river in combination with its groyne fields. The parameters studied involve groyne length, spacing, layout and crest elevation, while investigating three discharges from low flow to mean flow to a one-year flood. The aim of the study is hence to determine the sensitivity of these parameters and to find the groyne parameter which yields the maximum influence on flow field and morphodynamics.

2 STUDY SITES

The study was performed at two sites of the Danube River between Vienna, Austria and Bratislava, Slovakia: Witzelsdorf and Bad Deutsch-Altenburg (Fig. 1). Both reaches are located in the National Park "Donau Auen" (Danube Alluvial Zone National Park). This area comprises a free-flowing section of the Danube River of approximately 40 km in length, which was however heavily regulated in the 19th century (Hohensinner et al., 2004). Due to a sediment deficit from upstream, the section suffers from an ongoing river bed incision of around 2 to 3.5 cm per year; in connection with this, several oxbow lakes are no longer connected frequently, leading to ecological degradation, and also navigation is affected due to insufficient water depths during low flow periods. Therefore a river engineering and restoration project has been initiated that aims at a solution for all of these aforementioned problems by stabilizing the river bed, reconnecting oxbows, increasing sedimentation in the river by initiating lateral erosion processes, and improving navigation conditions and ecology by modifying groynes. Within the river restoration project, a comprehensive field monitoring campaign has been conducted since the year 2005, which forms the data base for the numerical study presented in this paper.

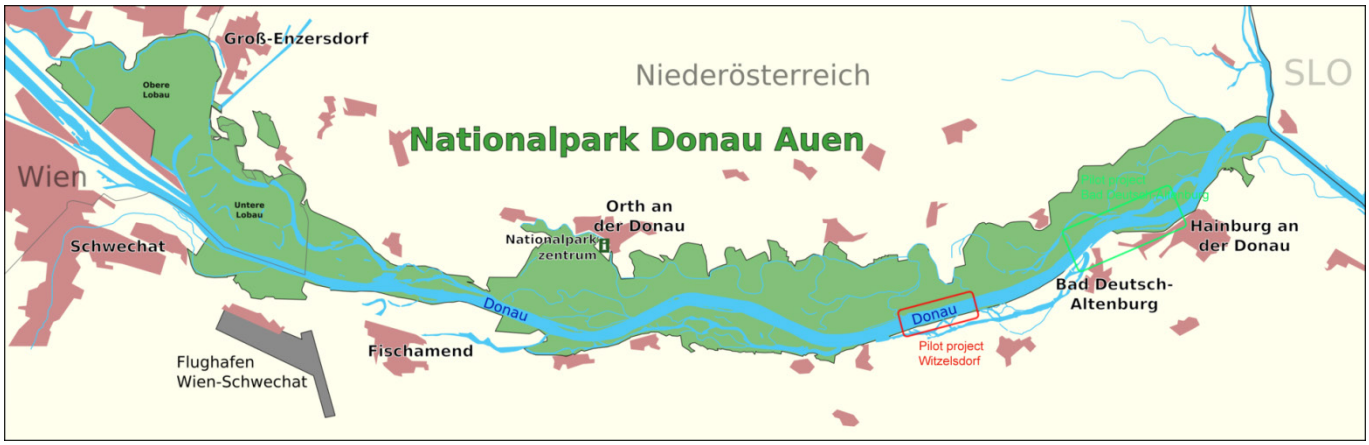

Figure 1. Location of the study sites.

The study reach of the pilot project Witzelsdorf (including an approach section required for numerical modelling) is located between river km 1891 and 1894. The analogous study reach of pilot project Bad Deutsch-Altenburg ranges from river km 1884 to 1888. In both reaches, alternative groyne layouts were applied in nature in recent years. With the overall outcomes from Bad Deutsch-Altenburg being generally comparable to those from the Witzelsdorf reach, this paper hence focuses on the results from Witzelsdorf.

Three characteristic discharges were studied: regulated low flow (RNQ; 94% probability of exceedance) with a discharge of 980 m^3s^{-1}, mean flow (MQ) with a discharge of 1930 m^3s^{-1} and highest navigable flow (HSQ; 1% probability of exceedance) with a discharge of 5130 m^3s^{-1}. The average river width at the study site Witzelsdorf amounts to approximately 300 m. Grain sizes in the bed of this section of the Danube River are characterized by an arithmetic mean diameter of d_m = 24 mm, a median diameter of d_{50} = 20 mm and a diameter d_{90} = 49 mm. Sediment samples in groyne fields and near the river banks, which were taken during the course of the measurement campaign, in part exhibit substantially finer grain size characteristics.

Measures completed in recent years at the study site Witzelsdorf are shown in Fig. 2. The original 8 groyne structures in orthogonal layout were removed and replaced by 4 new attracting groynes, intended

for deliberately increasing morphodynamics along the river bank. This process was supported by the removal of the bank protection over a length of 1.2 km. Moreover, a guiding wall upstream of the groyne array was lowered to increase dynamics during medium flow conditions. As an additional feature the bases of all four new groynes were lowered in order to provide a by-pass reach, intended for allowing juvenile fish to pass the section more easily and reduce sedimentation in the groyne fields.

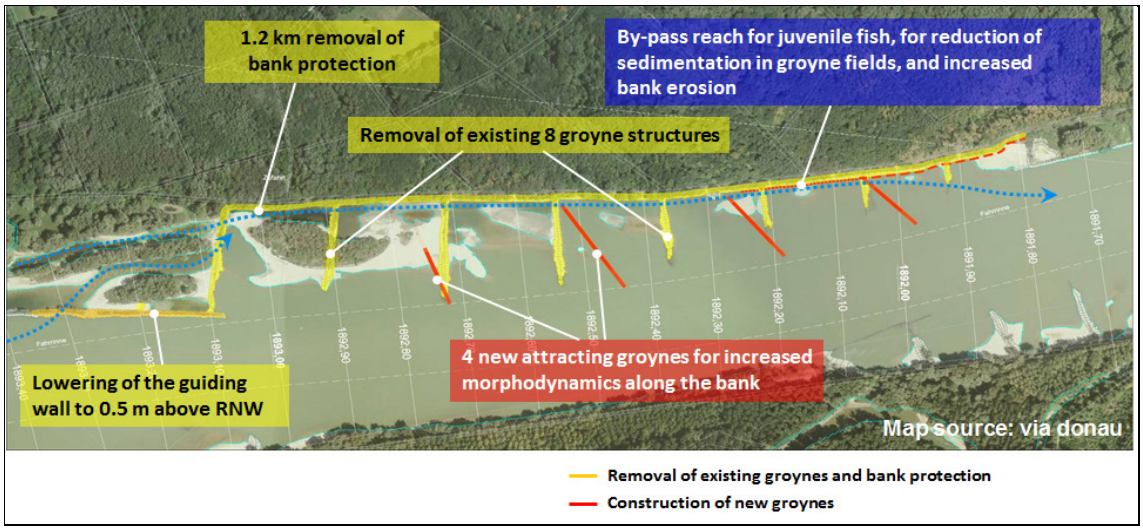

Figure 2. Measures completed at the Witzelsdorf study site.

3 NUMERICAL MODELS

3.1 *Hydrodynamic code RSim-3D*

The three-dimensional hydrodynamic model RSim-3D (Tritthart, 2005) solves the Reynolds-averaged Navier-Stokes equations on a mesh composed of arbitrary polyhedrons by means of the Finite Volume method (Tritthart and Gutknecht, 2007). A second order upwind scheme is employed for the interpolation of convective fluxes at cell boundaries. The coupling of pressure and velocity fields is performed by means of the SIMPLE algorithm in a generalized formulation following Davidson (1996). Turbulence is modelled using a standard two-equation k-ε closure (Launder and Spalding, 1974). The position of the free water surface elevation is derived from the computed pressure field in an iterative process.

3.2 *Sediment transport code iSed*

The integrated sediment transport model iSed (Tritthart et al., 2011) is capable to be coupled with external 2D or 3D hydrodynamic codes which in turn provide water depths, flow velocities and bed shear stresses as input for sediment transport and morphodynamics calculations. The model can handle different computation mesh types, ranging from triangular or quadrilateral cells in 2D to hexahedral or polyhedral cells in 3D. According to the actual processes occurring in sediment transport, suspended load and bed load are calculated separately from each other, consequently allowing the user to calculate only the transport process which is dominant for a specific application situation.

3.2.1 *Bedload transport*

The iSed model contains both uniform and non-uniform variants of the empirical transport equations by Meyer-Peter and Müller (1948), Egiazaroff (1965) and van Rijn (1984). Hiding-exposure (HE) corrections are available for the non-uniform transport equations, ranging from the classical HE correction of Einstein (1950) to the concept of calculating a representative diameter for every grain size fraction separately as introduced by Parker (1990). In this study, a non-uniform formulation of the transport equation after Meyer-Peter and Müller (1948) was used together with the HE correction by Einstein (1950):

$$q_{s,i} = p_i c_{MP} \sqrt{\frac{\rho_s - \rho}{\rho} g d_i^3 \left[\left(\frac{d_i}{d_{ref}} \right)^{\alpha} \frac{u_*'^2}{\frac{\rho_s - \rho}{\rho} g d_i} - \theta_{c,MP} \right]^3} \quad (1)$$

Herein, $q_{s,i}$ denotes the bed load transport capacity for fraction i, p_i is the mass fraction occupied by grain size i in the sediment mixture, c_{MP} a constant ($c_{MP} = 8.0$ according to Meyer-Peter and Müller (1948)), ρ_s the sediment density, ρ the density of water, g the gravitational acceleration, d_i the mean diameter of the sediment fraction i, d_{ref} a reference diameter which is assumed to be equal to the mean diameter ($d_{ref} = d_m$), and u_*' the grain-related shear velocity.

Hiding and exposure is governed by the exponent α which must be calibrated for each study case and takes values in the range of 0 to 1. The critical mobility parameter $\theta_{c,MP}$ was determined as $\theta_{c,MP} = 0.047$ by Meyer-Peter and Müller (1948). Later works, however, proposed $c_{MP} = 5.0$ and $\theta_{c,MP} = 0.050$ (Hunziker, 1995) or $c_{MP} = 4.93$ and $\theta_{c,MP} = 0.047$ (Wong and Parker, 2006). In accordance with previous experience at Austrian rivers (Habersack and Laronne, 2002), this study follows Hunziker's (1995) recommendation as far as $c_{MP} = 5.0$ is concerned, while treating $\theta_{c,MP}$ as calibration parameter.

3.2.2 *Suspended load transport*

Transport of suspended sediment is calculated in 2D; if a three-dimensional flow field is provided by the hydrodynamic code, it is depth-averaged for the purpose of suspended load calculations. The transport is described by a two-dimensional equation of convection-diffusion type, which includes an exchange term to account for the interaction with the river bed:

$$\frac{\partial c}{\partial t} + \frac{\partial (u_1 c)}{\partial x_1} + \frac{\partial (u_2 c)}{\partial x_2} = \frac{\partial}{\partial x_1}\left(K_t \frac{\partial c}{\partial x_1} \right) + \frac{\partial}{\partial x_2}\left(K_t \frac{\partial c}{\partial x_2} \right) + \left(s_{dep} - s_{ero} \right) \tag{2}$$

In Equation (2), c denotes the suspended sediment concentration, u_i the flow velocities in the corresponding coordinate directions x_i, K_t the depth-averaged diffusion coefficient, and t the time. s_{dep} is the deposition flux and s_{ero} the erosion flux with respect to the sediment layer at the river bed. The deposition flux is calculated for every size fraction i according to van Rijn (1984), while the erosion flux follows the relation proposed by Garcia and Parker (1991). Equation (2) is solved using a Finite Volume technique for arbitrary meshes, analogous to the solution algorithm used in the RSim-3D hydrodynamic model and detailed in Tritthart and Gutknecht (2007).

3.2.3 *Morphodynamics*

The evolution of the river bed elevation over time at every computation node follows the Exner equation:

$$\left(1 - n_p\right)\frac{\partial z_i}{\partial t} + \frac{\partial q_{si,x}}{\partial x} + \frac{\partial q_{si,y}}{\partial y} = s_{dep,i} - s_{ero,i} \tag{3}$$

In Equation (3), z_i denotes the vertical change in the bed elevation due to sediment transport processes in the fraction i; $q_{si,x}$ and $q_{si,y}$ represent the bedload transport rate, split into the coordinate directions x and y, according to the direction of the near-bed flow vector. n_p is the pore content of the sediment. The exchange term on the right-hand side of Equation (3) represents the balance between deposition and erosion flux due to suspended sediment transport and takes a value of zero if suspended sediment transport is not relevant for bed evolution. The near-bed flow vector is corrected for the effect of a transverse sloping bed following the relation proposed by Ikeda (1988). The Exner equation is solved applying the Finite Volume Method on a control volume surrounding the computation node, yielding the vertical bed level changes for every grain size fraction.

3.2.4 *Grain sorting*

The iSed model employs an exchange layer concept, thus all mixing processes take place in the top sediment layer. The width of this layer, which according to experience is usually in the range of one to four large gravels (i.e. d_{90} to 4 x d_{90}), is a model calibration parameter and influences the coarsening and fining of the bed sediment due to erosion and deposition, respectively. In case of erosion, sediment from lower subsurface layers is added to the mixing layer; if deposition is taking place, the deposited material is added instead, consequently yielding a new grain size distribution by evaluating the sorting equation detailed in Tritthart et al. (2011).

3.3 *Model setup, calibration and validation*

The digital terrain elevation model (DEM) used as basis for the study in Witzelsdorf was composed from single-beam and multi-beam bathymetric measurements performed after finalizing the construction works

in February/March 2010. Single-beam data was available in a cross section distance of 25 to 50 m. Elevation data obtained from a LIDAR terrestrial scan performed also in February 2010 was used for completing the DEM in the bank zones. Four further DEMs for the purpose of calibration and validation of the hydrodynamic and morphodynamic models were composed from bathymetric data measured in April 2009, August 2009, June 2010 and October 2011.

A computation mesh consisting of approximately 26.000 two-dimensional regions with mostly hexagonal base shapes was created, including mesh refinements near groyne structures and in bank zones. Following previous experience at the Danube River (e.g. Tritthart et al., 2009), a vertical mesh segmentation of six layers was selected, resulting in a total of 156.000 cells for the study site Witzelsdorf. The calibration of the hydrodynamic model was performed using a catalogue of official water surface elevations published by the waterways authority (KWD 2010) and the results of flow velocity measurements by ADCP technique. The result of the calibration process yielded a bed roughness value of $k_s = 0.03$ m for the river bed. The model was successfully validated using ADCP measurements at a discharge different from the one used for calibration.

Six grab samples of river bed sediment were taken in October 2009; moreover, surface and subsurface samples at three locations in the groyne fields were taken by hand. From this information, a sediment cover for the iSed model was composed, separated in a surface layer of 0.20 m thickness and a subsurface layer of 0.80 m. In the river bed, the Kriging interpolation method was applied in order to obtain a smooth transition between the grain size distributions of the grab samples. The sampled grain size distributions of the groyne fields and bank zones were directly assigned without further interpolation. Bedload and suspended load input were sampled qualitatively and quantitatively for three discharges during a measurement campaign from a vessel; from this information a sediment rating curve was constructed and used to obtain the upstream boundary condition for the sediment transport model. As mentioned before, calibration and validation of the model were performed successfully using DEMs at different points in time.

In order to compare the different groyne variants, the sediment transport model was run in quasi-steady calculation mode for each of the characteristic discharges RNQ, MQ and HSQ (see section 2) for a duration of 30 days.

4 GROYNE VARIANTS

After completion of the construction works at the Witzelsdorf study site, four attracting groynes in an approximate spacing of twice the groyne length, all equipped with lowered bases, constitute the status quo. The numerical study considered the following variants different from the current status: (i) orthogonal groyne layout, (ii) repelling groyne layout, (iii) groyne spacing of 1x the average groyne length, (iv) groyne spacing of 3x the average groyne length, (v) length increase of groynes by 20%, (vi) length decrease of groynes by 20%, (vii) increase of crest elevation by 0.4 m. Fig. 3 provides a visualization of these variants. In further computations, the effect of groynes without lowered bases and modifications of the crest elevation of the upstream guiding wall (Fig. 2) were tested.

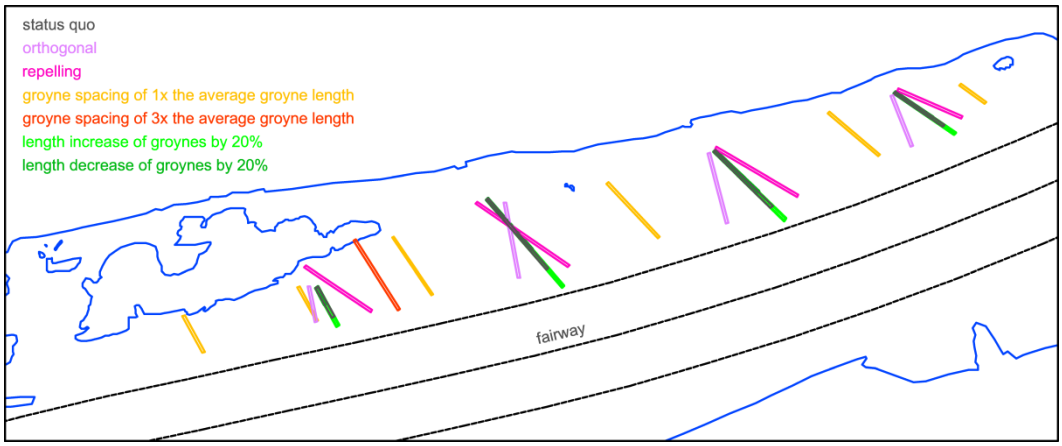

Figure 3: Schematic visualization of the groyne variants tested in the numerical study.

5 RESULTS AND DISCUSSION

The groyne variants were assessed in terms of their effect on (a) the flow velocities in the fairway (center area) of the river, (b) the shear stress patterns, (c) the water surface elevations, and (d) the resulting morphodynamic impact (sedimentation or erosion patterns at the river bed). In addition, as a proxy for the ecological influence the changes of the flow field within the groyne fields were analyzed using particle tracing methodology. For all parameters except the particle tracing analyses, maps of differences between the variants and the status quo (in the following denoted as reference condition) were created. Due to space constraints, only selected results can be presented in this paper, however the summary result Table 1 at the end of section 5 provides a synthesis of the results obtained.

5.1 *Results of the respective groyne variants*

5.1.1 *Orthogonal and repelling groyne layouts*

In general, groynes in orthogonal layout were found to lead to similar hydrodynamic and morphodynamic characteristics as compared to the reference condition. Most parameters have a slight tendency to increase, which can be reasoned by the somewhat larger flow constriction that is caused by the rotation of the groynes into orthogonal position while keeping their length constant. The largest influence is yielded on the water surface elevation, which increases notably during mean flow conditions.

The results also showed that overall characteristics of repelling groynes as compared to attracting ones are rather similar, besides the fact that lower flow velocities and shear stresses near the bank – which lead to a stabilizing effect – give the groyne structure a different purpose than the one which was intended in the project. Most notable though is a substantial reduction of water surface elevations during flood conditions, as compared to the reference condition.

5.1.2 *Groyne spacing*

A reduction of the groyne spacing to 1x the groyne length was found to yield a large increase in all hydrodynamic parameters – including water surface elevations – under all discharge conditions.

A local increase of flow velocities in the main channel during mean flow conditions (MQ) between 0.2 and 0.5 ms^{-1} leads to shear stress increases in the range of 2 to 5 Nm^{-2} (Fig. 4a). This in turn gives rise to substantial erosive processes which are predicted by the morphodynamics code to be over 0.15 m larger within 30 days of modelling time, compared with the reference condition (Fig. 4b). At the same time, sedimentation in the groyne fields was increasing.

An increase of the groyne spacing to 3x the groyne length was not found to exhibit any specific trend, however in general the differences in hydrodynamic conditions are comparably small. At least for low flow discharges bed level differences showed a tendency towards more sedimentation.

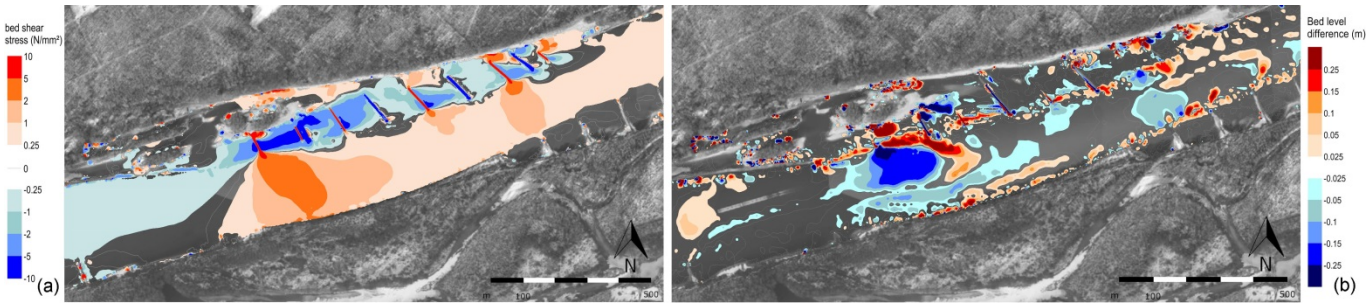

Figure 4: (a) Bed shear stress differences, (b) difference of differences (DoD) of bed level changes, between 1x average groyne length and reference condition for MQ.

5.1.3 *Groyne length*

An increase of the groyne length by 20% was found to lead to an increase in flow velocities, bed shear stresses and water surface elevations. This consequently results in larger erosion depths throughout the study reach.

In turn, the hydrodynamic patterns of a groyne length decrease by 20% showed a general decrease of flow velocities and bed shear stresses. Expectedly the morphodynamic simulations predicted larger sedimentation in the modelling domain, as compared to the reference condition.

5.1.4 *Crest elevation*

Particularly for mean flow conditions (MQ), an increase of the crest elevation by 0.4 m led to extraordinarily higher flow velocities and bed shear stresses, which exceeded those of all other variants.

Flow velocities increased between 0.1 and 0.2 ms-1 throughout most of the fairway within the study site and bed shear stresses between 2 and 5 Nm^{-2} in the same area. (Fig. 5a). From the shear stress difference map it also becomes obvious that more flow is passing the groynes with elevated crests on both sides, thus leading to a substantial increase in bank-near flow velocities and bed shear stress. Moreover, also the water surface elevation increased by a large amount. The resulting differences in erosive processes are shown in Fig. 5b and amount to 0.10 – 0.15 m larger erosion in vast areas of the main channel.

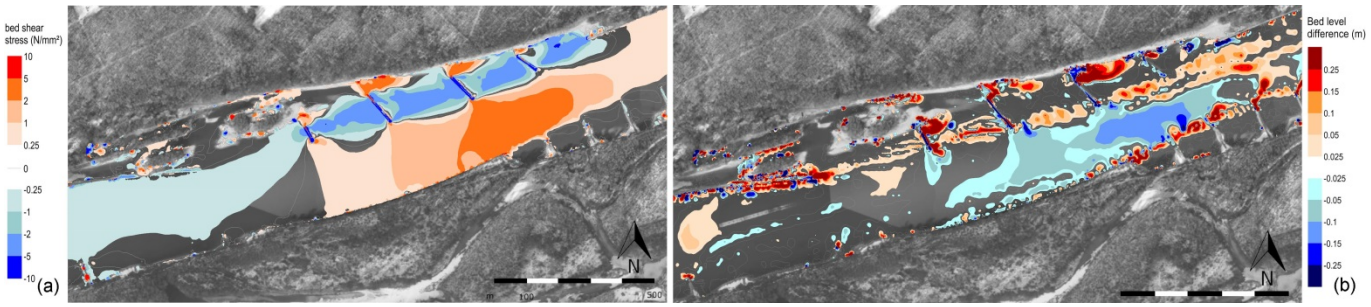

Figure 5: (a) Bed shear stress differences, (b) difference of differences (DoD) of bed level changes, between increased crest elevation and reference condition for MQ.

5.1.5 *Ecological aspects*

During low flow conditions, groyne fields in the reference condition exhibit one large gyre that is additionally propelled by the flow over the lowered groyne base. This pattern is visible for most variants, except for the single-spaced groyne layout, which often does not allow even a single gyre to form completely – thus increasing water ages – and the triple-spaced layout, which allows two counter-rotating gyres to form. Hence, mass exchange between main river channel and groyne fields will be positively influenced with rising groyne spacing.

5.2 *Overall assessment*

Table 1 summarizes the results of the hydrodynamic and morphodynamic computations. Therein, arrows pointing upwards denote an increase of the parameter, while downward arrows indicate a decrease. The number of arrows represents the magnitude of the increase or decrease of the parameter compared to the reference condition. An arrow pointing in both directions indicates that both effects are present, while an approximate-equal sign denotes parameters almost without effect. A minus sign is used if a variant does not have any effect at all for a given discharge.

Table 1. Summary of the influence of the groyne variants on hydrodynamics and morphodynamics, compared to reference

	Flow velocity			Bed shear stress			Water surface elev.			Bed level change		
Groyne variants	RNQ	MQ	HSQ	RNQ	MQ	HSQ	RNQ	MQ	HSQ	RNQ	MQ	HSQ
Orthogonal groynes	≈	↑	≈	↑	↑	↑	≈	↑↑	↓	≈	≈	≈
Attracting groynes	≈	↑	≈	≈	↑	↑	≈	↑	↓↓	≈	≈	↕
Spacing 1x length	↑↑↑	↑↑↑	↑↑	↑↑↑	↑↑↑	↑↑	↑↑	↑↑↑	↑	↓↓	↓↓↓	↓↓↓↓
Spacing 3x length	↕	↑	≈	↕	↑	↕	↕	↑	↓↓	↑↑	↓↓	↕
Increased length	↑↑	↑↑	≈	↑↑	↑↑	↑	↕	↑↑	≈	↓↓	↓	↓↓
Decreased length	↓	↓	≈	↓↓	↕	↓	↓	≈	↓↓	↑	↑	↑↑
Increased elevation	-	↑↑↑↑	↑	-	↑↑↑↑	↑	-	↑↑↑↑	≈	-	↓↓↓	↓↓

6 CONCLUSIONS

Several different groyne variants were studied numerically and analyzed according to their influence on hydrodynamics, morphodynamics and ecological criteria. It was found that an increase of the groyne length as well as a decrease of the groyne spacing lead to rising water levels. However, these measures also result in river bed erosion and increasing water ages in groyne fields due to reduced exchange processes. In turn, sedimentation in the fairway is obtained by an increase of the groyne spacing and a reduction

of the groyne length. This also corresponds to an increase of mass exchange between river and groyne fields due to the occurrence of two gyres. Moreover, it was found that the highest sensitivity of all groyne parameters in terms of morphodynamic processes is exhibited by the crest elevation. Thus, an optimization of the crest elevation is essential for achieving the aim of a dynamic equilibrium of the river bed.

ACKNOWLEDGMENT

The authors thank Johannes Steinkellner and Andreas Tauer for their contributions during their respective master theses as well as viadonau for their kind support and contribution of data to this study. Moreover, the financial support by the Federal Ministry of Economy, Family and Youth and the National Foundation for Research, Technology and Development is gratefully acknowledged.

REFERENCES

Alauddin, M., Tsujimoto, T. (2012). Optimum configuration of groynes for stabilization of alluvial rivers with fine sediments. Int. J. Sed. Res., Vol. 27, No. 2, pp. 158-167.

Biron, P.M., Robson, C., Lapointe, M.F., Gaskin, S.J. (2005). Three-dimensional flow dynamics around deflectors. River Res. Appl., Vol. 21, pp. 961-975.

Davidson, L. (1996). A pressure correction method for unstructured meshes with arbitrary control volumes. Int. J. Numer. Meth. Fluids, Vol. 22, pp. 265-281.

Egiazaroff, I.V. (1965). Calculation of nonuniform sediment concentration. J. Hydraulics Div. ASCE, Vol. 91, pp. 225-247.

Einstein, H.A. (1950). The bed-load function for sediment transportationin open channel flow. Technical Bulletin 1026. U.S. Department of Agriculture, Washington, D.C.

Garcia, M., Parker, G. (1991). Entrainment of bed sediment into suspension. J. Hydraulic Eng., Vol. 117, pp. 414-435.

Habersack, H., Laronne, J.B. (2002). Evaluation and improvement of bed load discharge formulas based on Helley-Smith Sampling in an Alpine gravel bed river. J. Hydraulic Eng., Vol. 128, No. 5, pp. 484-499.

Henning, M., Hentschel, B. (2013). Sedimentation and flow patterns induced by regular and modified groynes on the River Elbe, Germany. Ecohydrology, Vol. 6, No. 4, pp. 598-610.

Hohensinner, S., Habersack, H., Jungwirth, M., Zauner, G. (2004). Reconstruction of the characteristics of a natural alluvial river-floodplain system and hydromorphological changes following human modifications: the Danube River (1812-1991). River Res. Appl., Vol. 20, No. 1, pp. 25-41.

Hunziker, R.P. (1995). Fraktionsweiser Geschiebetransport. VAW Mitteilung 138. ETH Zürich, Switzerland.

Ikeda, S. (1988). Lateral bed load transport on side slopes. In: Civil engineering practice 2, Technomic Publishing Co., Lancaster PA, pp. 299-307.

Kang, J., Yeo, H., Kim, S., Ji, U. (2011). Experimental investigation on the local scour characteristics around groynes using a hydraulic model. Water and Environment Journal, Vol. 25, No. 2, pp. 181-191.

Launder, B.E., Spalding, D.B. (1974). The numerical computation of turbulent flows. Comp. Meth. Appl. Mech. Eng., Vol. 3, pp 269-289.

Lechner, A., Keckeis, H., Schludermann, E., Loisl, F., Humphries, P., Glas, M., Tritthart, M., Habersack, H. (2014). Shoreline configurations affect dispersal patterns of fish larvae in a large river. ICES J. Marine Science, Vol. 71, No. 4, pp. 930-942.

Meyer-Peter, E., Müller, R. (1948). Formulas for bed-load transport. Proc. 2nd IAHR Congress, Stockholm, Sweden, pp 39-64.

Ouillon, S., Dartus, D. (1997). Three-dimensional computation of flow around groyne. J. Hydraul Eng., Vol. 123, pp. 962-970.

Parker, G. (1990). Surface-based bedload transport relation for gravel rivers. J. Hydraul. Res., Vol. 28, No. 4, pp. 417-436.

Sukhodolov, A.N. (2014). Hydrodynamics of groyne fields in a straight river reach: insight from field experiments. J. Hydraul. Res., Vol. 52, No. 1, pp. 105-120.

Tritthart, M. (2005). Three-dimensional numerical modelling of turbulent river flow using polyhedral finite volumes. Wiener Mitteilungen Wasser-Abwasser-Gewässer, Vol. 193, 179 pp.

Tritthart, M., Gutknecht, D. (2007). Three-dimensional simulation of free-surface flows using polyhedral finite volumes. Engineering Applications of Computational Fluid Mechanics, Vol. 1, No. 1, pp. 1-14.

Tritthart, M., Liedermann, M., Habersack, H. (2009). Modelling spatio-temporal flow characteristics in groyne fields. River Res. Appl., Vol. 25, No. 1, pp. 62-81.

Tritthart, M., Schober, B., Habersack, H. (2011). Non-uniformity and layering in sediment transport modelling 1: flume simulations. J. Hydraul. Res., Vol. 49, No. 3, pp. 325-334.

Uijttewaal, W.S.J., Lehmann, D., van Mazijk, A. (2001). Exchange processes between a river and its groyne fields: model experiments. J. Hydraul. Eng., Vol. 127, pp. 928-936.

Uijttewaal, W.S.J. (2005). Effects of groyne layout on the flow in groyne fields: laboratory experiments. J. Hydraul. Eng., Vol. 131, pp. 782-791.

van Rijn, L.C. (1984). Sediment transport 1: Bed load transport. J. Hydraul. Eng., Vol. 110, No. 10, pp. 1431-1456.

Vierlingh A. (1576). Tractaet van dyckagie. Reprint by De Hullu, J., Verhoeven, A.G. (eds). ´s Gravenhagen, The Netherlands.

Wong, M., Parker, G. (2006). Reanalysis and correction of bed-load relation of Meyer-Peter and Müller using their own database. J. Hydraulic Eng., Vol. 132, No. 11, pp. 1159-1168.

Yossef, M.F.M., de Vriend, H.J. (2011). Flow Details near River Groynes: Experimental Investigation. J. Hydraul. Eng., Vol. 137, No. 5, pp. 504-516.